JACS
JOURNAL OF THE AMERICAN CHEMICAL SOCIETY

Communication

pubs.acs.org/JACS

Photo-induced Proton-Coupled Electron Transfer Reactions of Acridine Orange: Comprehensive Spectral and Kinetics Analysis

Thomas T. Eisenhart and Jillian L. Dempsey*

Department of Chemistry, University of North Carolina, Chapel Hill, North Carolina 27599-3290, United States

Supporting Information

ABSTRACT: The triplet excited state of acridine orange (^{3}*AO) undergoes a proton-coupled electron transfer (PCET) reaction with tri-*tert*-butylphenol (^{ttb}PhOH) in acetonitrile. Each of the reaction components possesses a spectroscopic signature, providing a rare opportunity to monitor the individual proton transfer, electron transfer, and H$^\bullet$-transfer components in parallel via transient absorption spectroscopy. This enhanced optical tracking, along with excited-state thermochemical analysis, facilitates assignment of the mechanism of excited-state PCET reactivity. ^{3}*AO is quenched via concerted proton–electron transfer (CPET) from ^{ttb}PhOH to form acridine radical (AOH$^\bullet$) and ^{ttb}PhO$^\bullet$ (k_{CPET} = 3.7 × 10^8 M^{-1} s^{-1}, KIE = 1.3). Subsequently, AOH$^\bullet$ reduces the phenoxyl radical (k_{ET} = 5.5 × 10^9 M^{-1} s^{-1}), forming AOH$^+$ and ^{ttb}PhO$^-$, followed by proton transfer (k_{PT} = 1.0 × 10^9 M^{-1} s^{-1}) to regenerate the starting reactants.

Proton-coupled electron transfer (PCET) processes are central to the conversion of small molecules to energy-rich fuels.[1,2] Harvesting solar energy to achieve these challenging transformations is an increasingly attractive option as the need for alternative energy resources becomes more pressing. Investigation of PCET in biological systems and in molecular models provides a general understanding of PCET processes between molecules in their electronic ground states,[1−6] but comparatively little is known about PCET reactions of electronically excited molecules.[7−9] In response, we are undertaking mechanistic studies to provide a comprehensive understanding of excited-state PCET reactions. Rationalizing how to integrate light absorption and H$^+$/e$^-$ transfer will facilitate the design of new systems that can effectively couple energy capture and conversion.

A great deal of research has focused on the thermal PCET reactions of phenol substrates, in part because of the importance of tyrosine radicals in biological systems such as photosystem II and ribonucleotide reductase.[1,2,4,5,10] As a result, the PCET thermochemistry for a great many phenols is well established, including parameters for concerted proton–electron transfer (CPET) and stepwise electron transfer–proton transfer (ET-PT) and proton transfer–electron transfer (PT-ET) pathways.[11] By coupling this information to excited-state reduction potentials (obtained via modified Latimer diagrams[12,13]) and excited-state pK_a values (determined from Förster cycles[14,15]), a thermochemical picture of excited-state PCET reactions can be developed.[8]

Here, we describe the detailed mechanistic study of a system that undergoes excited-state PCET followed by a thermal PCET reaction that yields the reactants in their electronic ground states. Our model system is based on acridine orange (AO), a Brønsted base and a mild excited-state oxidant that undergoes efficient intersystem crossing to a long-lived triplet state.[16,17] Some N-heterocyclic compounds are known to be photochemically active toward PCET reagents,[18−20] and herein we show that AO conforms to this reactivity pattern. Employing AO, we photo-trigger the PCET oxidation of tri-*tert*-butylphenol (^{ttb}PhOH) in CH_3CN and track the reaction intermediates with time-resolved spectroscopy. ^{3}*AO can react with ^{ttb}PhOH through a concerted pathway or one of several stepwise PCET reaction pathways (Scheme 1). The strong

Scheme 1. PCET Square Scheme Incorporating Ground- and Excited-State Reactivity

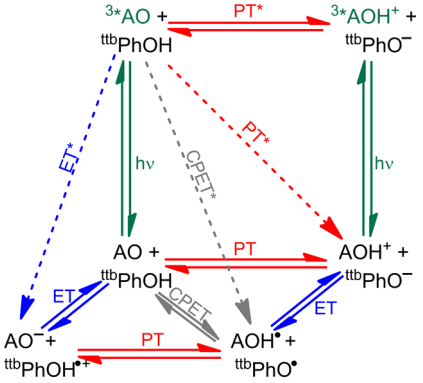

absorption features of AO (λ_{max} = 425 nm, ε = 12 500 M^{-1} cm^{-1}) and the corresponding acridinium (AOH$^+$, λ_{max} = 495 nm, ε = 31 250 M^{-1} cm^{-1}) provide spectroscopic handles for determining the AO protonation states; the oxidation states of these species can also be assessed optically (Figure S1, Supporting Information). Analysis of the transient absorption (TA) spectra and corresponding kinetics traces provides a complete picture of the light-induced PCET oxidation of phenol and the subsequent thermal reaction.

In the absence of reactive O–H bonds, TA spectra of AO in CH_3CN (Figure S2) recorded at time intervals between 100 ns and 100 μs following excitation (λ_{ex} = 425 nm) reveal three features: new absorptions centered at 410 and 540 nm

Received: June 8, 2014

   dx.doi.org/10.1021/ja505755k | J. Am. Chem. Soc. XXXX, XXX, XXX−XXX

corresponding to the triplet excited state of (^{3}*AO) and a bleach centered at 435 nm due to the loss of the ground-state AO absorption. These transient features decay non-exponentially: ^{3}*AO undergoes first-order decay through a nonradiative process (k_{nr}), reacts through a triplet−triplet interaction (k_{TT}) to produce the corresponding radical cation (AO^+) and radical anion (AO^-), and is quenched by ground-state AO (k_s).[16,17,21] Transient features and decay rate constants determined from modeling single-wavelength kinetics traces are similar to those reported in water at pH 12 (Table S1, Figure S3).[17]

In the presence of ^{ttb}PhOH, we observe accelerated decay of the ^{3}*AO transient absorption features (410 and 540 nm) (Figure 1A). Between 100 ns and 10 μs, the blue absorption

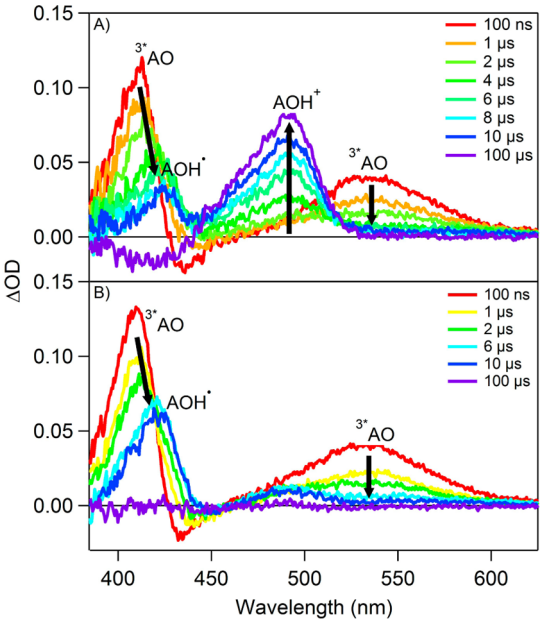

Figure 1. Transient difference spectra of (A) 40 μM AO and 1 mM ^{ttb}PhOH and (B) 40 μM AO and 3 mM TEMPOH in CH_3CN at selected time delays after laser excitation. λ_{ex} = 425 nm, 0.1 mM $[Bu_4N][PF_6]$.

feature undergoes a bathochromic shift to 425 nm. This new feature is consistent with the formation of a neutral acridine radical ($AOH^•$), the absorption spectrum (λ_{max} = 425 nm, $\varepsilon \geq$ 6500 M^{-1} cm^{-1}) of which was measured independently via reduction of AOH^+ in a spectroelectrochemical cell (Figure S4). The concurrent growth of a small signal at 400 nm indicates the formation of ^{ttb}PhO• (λ_{max} = 400, ε = 2120 M^{-1} cm^{-1}).[22] In the time interval 10−100 μs, the $AOH^•$ signal decays and a transient bleach centered at 425 nm, assigned to the loss of AO, appears on the high-energy side of the spectra. Most notably, the spectra recorded in the time interval 4−100 μs are dominated by the growth of a prominent feature at 495 nm, which is consistent with production of AOH^+.

For comparison, we also explored excited-state PCET reactivity of AO in the presence of 1-hydroxyl-2,2,6,6-tetramethylpiperidine (TEMPOH), a well-documented PCET reagent that favors CPET over stepwise mechanisms.[11] As for ^{ttb}PhOH, added TEMPOH quenches the triplet absorbance features of AO at 410 and 540 nm (Figure 1B). The appearance of $AOH^•$ (425 nm) is observed between 100 ns and 10 μs. The concurrent detection of TEMPO• is not expected (λ_{max} = 463 nm, ε = 10 M^{-1} cm^{-1}).[23] In contrast with the reactivity of ^{ttb}PhOH, no dominant signal at 495 nm appears. The signal corresponding to $AOH^•$ decays on the 100 μs time scale.

Optical detection of discrete intermediates aids evaluation of H^+/e^- transfer mechanisms for reactions between ^{3}*AO with ^{ttb}PhOH or TEMPOH. The mechanisms indicated in Schemes 2 and 3 are consistent with the spectral evidence for reaction

Scheme 2

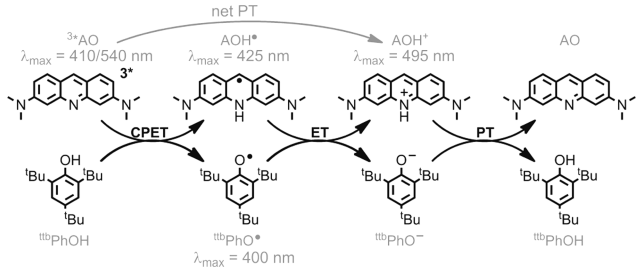

Scheme 3

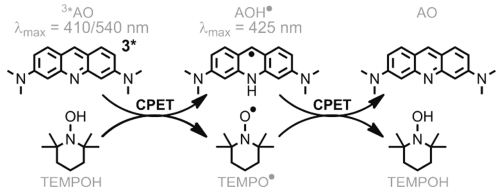

intermediates. ^{3}*AO is quenched by CPET from both ^{ttb}PhOH and TEMPOH to form ^{ttb}PhO• and TEMPO•, respectively, along with $AOH^•$. This reactivity is presumed to occur through a hydrogen-bonded encounter complex, consistent with previous reports of photo-induced PCET reactions in organic solvents.[24−26]

After formation of the excited-state CPET products, thermal back-PCET ensues to yield the ground-state reactants. Thermochemical analysis (see Supporting Information) indicates that ET-PT and CPET processes are both reasonable pathways for the reaction of ^{ttb}PhO• and $AOH^•$ because they circumvent high energy intermediates (in contrast, initial PT has ΔG°_{PT} = 49.9 kcal mol^{-1}). Spectral observation of the initial ET product (AOH^+) indicates the reaction proceeds via the stepwise ET-PT pathway. Specifically, the $AOH^•$ formed by excited-state CPET is a moderate reductant that can reduce ^{ttb}PhO• (ΔG°_{ET} = −20.8 kcal mol^{-1}), and accordingly, ET from $AOH^•$ to ^{ttb}PhO• proceeds to form AOH^+ and $^{ttb}PhO^-$, detected by the decay of the transient $AOH^•$ signal and the appearance of the AOH^+ absorption feature. Similar reactivity was noted for reactions of phenyl thiyl radical with 9-mesityl-10-methylacridinium, the former acting as an oxidant in a photoredox catalysis scheme.[27] The products of this sequential excited-state CPET−thermal ET sequence are equivalent to a net-PT process, reminiscent of reactivity proposed for ruthenium−phenol dyads.[24,28,29] Subsequently, AOH^+ and $^{ttb}PhO^-$ recombine via PT to form the ground-state reactants, detected by the decay of the AOH^+ signal.

By contrast, the thermal back-PCET reaction of $AOH^•$ and TEMPO• proceeds via CPET to form the ground-state reactants in the time interval 1−100 μs. This assignment is consistent with both spectral observations and the thermochemical preference of TEMPO• to react via CPET pathways (ΔG°_{CPET} = −21.7 kcal mol^{-1}, ΔG°_{ET} = +8.1 kcal mol^{-1}, ΔG°_{PT} = +50.1 kcal mol^{-1}). The diverging thermal reactivity of $AOH^•$

dx.doi.org/10.1021/ja505755k | J. Am. Chem. Soc. XXXX, XXX, XXX−XXX

with ^{ttb}PhO$^{\bullet}$ vs TEMPO$^{\bullet}$ is attributed to the different thermochemistry of the two systems.[11]

The spectral profiles of the AO-derived intermediates allows for detailed kinetics analyses. The quenching of ^{3}*AO by ^{ttb}PhOH was monitored by single wavelength TA at 560 nm (Figure 2). Quenching is enhanced with increasing concentrations of ^{ttb}PhOH, but the excited-state decay is non-exponential. A kinetics model based on Scheme 2 and accounting for the intrinsic decay pathways of AO (Scheme S1) was used to describe the photo-induced PCET reaction between AO and ^{ttb}PhOH and subsequent thermal reactivity. Intrinsic reactivity of ^{3}*AO (above) is described by rate constants k_{nr}, k_{TT}, and k_{S}, respectively. The presence of trace amounts of AOH^{+} in solution is accounted for by the independently measured rate constant k_{AOH} (4×10^{4} s^{-1}), which describes the relaxation of ^{3}*AOH^{+} (Figure S5). Excited-state CPET is described by k_{CPET}. Though not detectable at 560 nm, ET from AOH$^{\bullet}$ to ^{ttb}PhO$^{\bullet}$ (k_{ET}) and PT from AOH^{+} to ^{ttb}PhO^{-} (k_{PT}) complete the model. Rate constants for these processes were determined from kinetics traces recorded at 460 nm and are discussed below.

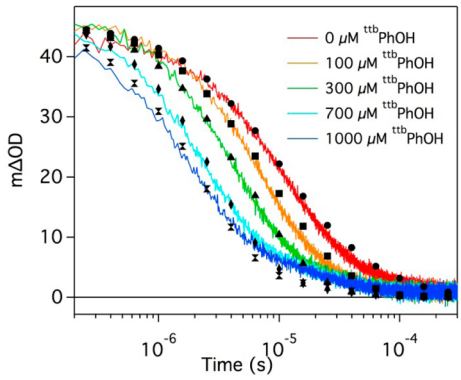

Figure 2. Kinetics traces (lines) of 40 μM AO with 0−1000 μM ^{ttb}PhOH in CH_3CN and the simulated spectra (markers). λ_{ex} = 425 nm, λ_{obs} = 560 nm, 0.1 M $[Bu_4N][PF_6]$.

Kinetics simulations were performed with a series of differential equations (Scheme S2) derived from the kinetics model described in Scheme S1. The rate law for the coupled reactions was solved numerically with an ordinary differential equations solver. Vectors describing initial concentrations of reactants, intermediates, and products, the time interval for analysis, and rate constants were provided as inputs to solve the initial value problem. The time-dependent concentration profiles produced for each species were translated to simulated TA difference spectra by applying the Beer−Lambert law and summing the absorbance values for each species. Rate constants were adjusted iteratively to simulate the kinetics traces for a series of five samples (0−1000 μM ^{ttb}PhOH) to obtain a self-consistent set of rate constants. Rate constants independently determined (k_{nr}, k_{TT}, k_{S}, k_{AOH}) for intrinsic decay pathways were fixed at these values in order to give the most accurate rate constants for the other processes.

The second-order rate constant determined for excited-state CPET is 3.7×10^{8} M^{-1} s^{-1}. The analogous reaction for ^{3}*AO and ^{ttb}PhOD is slightly slower ($k_{CDET} = 2.9 \times 10^{8}$ M^{-1} s^{-1}, KIE = 1.3) (Figure S6). This small, but non-negligible KIE is consistent with our assignment of CPET.[1,30] The second-order rate constant determined through kinetic simulations is a composite of the association constant for the formation of the hydrogen-bonded AO−phenol adduct and the first-order rate constant for intra-adduct CPET. Because of the complexity of the system, we cannot directly extract K_A and a first-order rate constant as has previously been done in luminescence quenching experiments.[24−26] Interpreting hydrogen bonding in the context of kinetics analysis is the focus of ongoing study.

These kinetic details, coupled with thermochemical analysis (see Supporting Information), support the proposed forward CPET, reverse ET-PT reaction sequence. An activation energy ($\Delta G^{\ddagger}$) in the range of +9.9−11.2 kcal mol^{-1} can be estimated from the k_{CPET} (based on the range of [^{ttb}PhOH] investigated).[11] Quenching of ^{3}*AO by ^{ttb}PhOH via an ET pathway is inconsistent with this barrier (ΔG°_{ET} = +23.1 kcal mol^{-1}). If PT from ^{ttb}PhOH to ^{3}*AO is not accompanied by excited-state deactivation (^{3}*AOH^{+} is formed initially, then subsequently relaxes to form AOH^{+}), initial PT has a negligible barrier (ΔG°_{PT} = +1.6 kcal mol^{-1}). Alternatively, if PT is coupled to excited-state deactivation of ^{3}*AO, the free energy change for PT (ΔG°_{PT} = −47.6 kcal mol^{-1}) indicates this pathway is highly exergonic, though the organic framework does not offer a clear mechanism for coupling relaxation.[31] However, for both of these initial PT pathways, the subsequent ET reaction between AOH^{+} and ^{ttb}PhO^{-} to form the net PCET products observed spectroscopically is substantially endergonic (ΔG°_{ET} = +20.8 kcal mol^{-1}), inconsistent with the observed $\Delta G^{\ddagger}$. Further, the large positive ΔG°_{ET} for the PT-ET pathway suggests that the excited-state PT intermediates AOH^{+} and ^{ttb}PhO^{-} should be detectable, but they are not observed. Rather, consistent with transient spectral measurements and the estimated barrier, ^{3}*AO is quenched by CPET (ΔG°_{CPET} = −26.8 kcal mol^{-1}) from ^{ttb}PhOH to form ^{ttb}PhO$^{\bullet}$ and acridine radical AOH$^{\bullet}$.

The appearance and subsequent reactivity of AOH^{+} were monitored at 460 nm as functions of AO (and, in turn, ^{3}*AO) concentration (Figure 3). Simulations of these kinetics traces per the model described above provides additional insight into the subsequent thermal ET and PT steps: ET from AOH$^{\bullet}$ to ^{ttb}PhO$^{\bullet}$ (k_{ET}) and PT from AOH^{+} to ^{ttb}PhO^{-} (k_{PT}). In this analysis, rate constants k_{nr}, k_{TT}, k_{S}, k_{AOH}, and k_{CPET} determined from simulations of 560 nm kinetics traces were fixed. The rate constant for k_{ET} is diffusion limited (5.5×10^{9} M^{-1} s^{-1}), consistent with the 900 mV driving force for ET (ΔG°_{ET} = −20.8 kcal mol^{-1}), and no KIE is observed, as expected.[11]

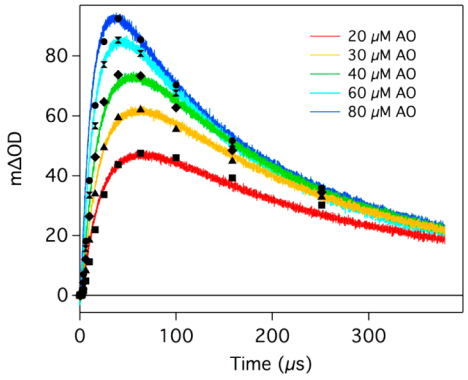

Figure 3. Kinetics traces (lines) of 20−80 μM AO with 500 μM ^{ttb}PhOH in CH_3CN and the simulated spectra (markers). λ_{ex} = 425 nm, λ_{obs} = 460 nm, 0.1 M $[Bu_4N][PF_6]$.

dx.doi.org/10.1021/ja505755k | J. Am. Chem. Soc. XXXX, XXX, XXX−XXX

Recombination of AOH^+ and $^{ttb}PhO^-$ via PT occurs with a rate constant of 1.0×10^9 M^{-1} s^{-1}, consistent with the large driving force (8.7 unit pK_a difference, $\Delta G^{\circ}_{PT} = -11.9$ kcal mol^{-1}).[11] No KIE is observed, as anticipated for diffusion-controlled bimolecular PT and consistent with related studies (Figure S7).[32]

In summary, we found that ^{3}*AO reacts with ^{ttb}PhOH and TEMPOH via excited-state CPET pathways. Excited-state CPET reactions of ^{3}*AO have not, to our knowledge, been previously observed. The ensuing reactivity of the CPET products is dictated by the thermodynamics of the respective systems: $AOH^{\bullet}$ reduces $^{ttb}PhO^{\bullet}$ but is not a potent enough reductant to reduce $TEMPO^{\bullet}$. Importantly, the unique spectroscopic signatures of the reactants, intermediates, and products enabled us to monitor each step of the photo-initiated and subsequent thermal reactions. The spectral evidence for the aforementioned reactivity is supported by kinetics modeling, thermochemical arguments, and H/D KIEs. This comprehensive picture of excited-state PCET reactivity provides new insight into the intimate coupling of light absorption with both proton and electron transfer. Harnessing this light-driven reactivity will pave new avenues to solar fuel production.

■ ASSOCIATED CONTENT

Supporting Information

Experimental details, spectrophotometric titrations, cyclic voltammograms, additional transient absorption spectra, additional kinetics traces, thermochemical calculations, and details of kinetic modeling. This material is available free of charge via the Internet at http://pubs.acs.org.

■ AUTHOR INFORMATION

Corresponding Author

dempseyj@email.unc.edu

Notes

The authors declare no competing financial interest.

■ ACKNOWLEDGMENTS

This work was supported by the University of North Carolina at Chapel Hill. We thank Prof. Jeffrey J. Warren and Dr. Jay R. Winkler for insightful discussions and Dr. M. Kyle Brennaman for experimental assistance. This research made use of instrumentation funded by the UNC EFRC: Center for Solar Fuels, an Energy Frontier Research Center supported by the U.S. Department of Energy, Office of Science, Office of Basic Energy Sciences, under award no. DE-SC0001011.

■ REFERENCES

(1) Weinberg, D. R.; Gagliardi, C. J.; Hull, J. F.; Murphy, C. F.; Kent, C. A.; Westlake, B. C.; Paul, A.; Ess, D. H.; McCafferty, D. G.; Meyer, T. J. *Chem. Rev.* **2012**, *112*, 4016−4093.
(2) Costentin, C.; Robert, M.; Savéant, J.-M *Chem. Rev.* **2010**, *110*, PR1−PR40.
(3) Mayer, J. M.; Rhile, I. J.; Larsen, F. B.; Mader, E. A.; Markle, T. F.; DiPasquale, A. G. *Photosynth. Res.* **2006**, *87*, 3−20.
(4) Dempsey, J. L.; Winkler, J. R.; Gray, H. B. *Chem. Rev.* **2010**, *110*, 7024−7039.
(5) Costentin, C.; Robert, M.; Savéant, J.-M. *Acc. Chem. Res.* **2010**, *43*, 1019−1029.
(6) Stubbe, J.; Nocera, D. G.; Yee, C. S.; Chang, M. C. Y. *Chem. Rev.* **2003**, *103*, 2167−2201.
(7) Wenger, O. S. *Acc. Chem. Res.* **2013**, *46*, 1517−1526.
(8) Wenger, O. S. *Coord. Chem. Rev.* **2014**, DOI: 10.1016/j.ccr.2014.03.025.
(9) Gagliardi, C. J.; Westlake, B. C.; Kent, C. A.; Paul, J. J.; Papanikolas, J. M.; Meyer, T. J. *Coord. Chem. Rev.* **2010**, *254*, 2459−2471.
(10) Hammarström, L.; Styring, S. *Energy Environ. Sci.* **2011**, *4*, 2379−2388.
(11) Warren, J. J.; Tronic, T. A.; Mayer, J. M. *Chem. Rev.* **2010**, *110*, 6961−7001.
(12) Rehm, D.; Weller, A. *Isr. J. Chem.* **1970**, *8*, 259−271.
(13) Juris, A.; Balzani, V.; Barigelletti, F.; Campagna, S.; Belser, P.; von Zelewsky, A. *Coord. Chem. Rev.* **1988**, *84*, 85−277.
(14) Forster, T. *Z. Elektrochem.* **1950**, *54*, 531−535.
(15) Grabowski, Z. R.; Rubaszewska, W. *J. Chem. Soc., Faraday Trans. 1* **1977**, *73*, 11−28.
(16) Chan, M. S.; Bolton, J. R. *Photochem. Photobiol.* **1981**, *34*, 537−547.
(17) Kellmann, A. *Photochem. Photobiol.* **1971**, *14*, 85−93.
(18) Beak, P.; Messer, W. In *Organic Photochemistry*, Vol. *2*; Chapman, O., Ed.; Marcel Dekker: New York, 1969; pp 117−167.
(19) Kuzmin, V. A.; Levin, P. P.; Belyaev, A. B. *Bull. Acad. Sci. USSR, Div. Chem. Sci.* **1989**, 165−167.
(20) Ford, W. E.; Rodgers, M. A. J. *J. Photochem. Photobiol. A: Chem.* **1991**, *59*, 73−80.
(21) Kellmann, A. *Photochem. Photobiol.* **1974**, *20*, 103−108.
(22) Manner, V. W.; Markle, T. F.; Freudenthal, J. H.; Roth, J. P.; Mayer, J. M. *Chem. Commun.* **2008**, 256−258.
(23) Nakahara, K.; Iwasa, S.; Iriyama, J.; Morioka, Y.; Suguro, M.; Satoh, M.; Cairns, E. J. *Electrochim. Acta* **2006**, *52*, 921−927.
(24) Kuss-Petermann, M.; Wenger, O. S. *J. Phys. Chem. A* **2013**, *117*, 5726−5733.
(25) Pizano, A. A.; Yang, J. L.; Nocera, D. G. *Chem. Sci.* **2012**, *3*, 2457−2461.
(26) Concepcion, J. J.; Brennaman, M. K.; Deyton, J. R.; Lebedeva, N. V.; Forbes, M. D. E.; Papanikolas, J. M.; Meyer, T. J. *J. Am. Chem. Soc.* **2007**, *129*, 6968−6969.
(27) Nguyen, T. M.; Nicewicz, D. A. *J. Am. Chem. Soc.* **2013**, *135*, 9588−9591.
(28) Bronner, C.; Wenger, O. S. *Phys. Chem. Chem. Phys.* **2014**, *16*, 3617−3622.
(29) Chen, J.; Kuss-Petermann, M.; Wenger, O. S. *Chem.—Eur. J.* **2014**, *20*, 4098−4104.
(30) Alligrant, T. M.; Alvarez, J. C. *J. Phys. Chem. C* **2011**, *115*, 10797−10805.
(31) Dempsey, J. L.; Winkler, J. R.; Gray, H. B. *J. Am. Chem. Soc.* **2010**, *132*, 16774−16776.
(32) Irebo, T.; Zhang, M.-T.; Markle, T. F.; Scott, A. M.; Hammarström, L. *J. Am. Chem. Soc.* **2012**, *134*, 16247−16254.